Particle acceleration at pulsar wind termination shocks revisited: shear, reconnection and giant plasmoids

Benoît Cerutti[a,*] **and Gwenael Giacinti**[b,c,d]

[a]*Univ. Grenoble Alpes, CNRS, IPAG, 38000 Grenoble, France*

[b]*Max-Planck-Institut für Kernphysik, Postfach 103980, 69029 Heidelberg, Germany*

[c]*Tsung-Dao Lee Institute, Shanghai Jiao Tong University, Shanghai 201210, P. R. China*

[d]*School of Physics and Astronomy, Shanghai Jiao Tong University, Shanghai 200240, P. R. China*
  E-mail: benoit.cerutti@univ-grenoble-alpes.fr,
gwenael.giacinti@mpi-hd.mpg.de, gwenael.giacinti@sjtu.edu.cn

Particle acceleration in relativistic shocks is quenched in the presence of a transverse magnetic field, even for a moderately low upstream magnetization. Pulsar wind nebulae form downstream of an ultra-relativistic magnetized shock; yet these objects are one of the most efficient particle accelerators known in the Galaxy. We propose that the key to this striking discrepancy lies in the anisotropic nature of the magnetic field profile in the pulsar wind. Using particle-in-cell simulations, we show that it has a dramatic impact on the structure and evolution of the shock. The formation of a current sheet in the equatorial plane, combined with a large-scale velocity shear flow lead to strong plasma turbulence and efficient non-thermal particle acceleration near the Bohm limit. The interplay between these processes may power the bright synchrotron nebula surrounding pulsars and possibly the puzzling Crab gamma-ray flares. Another important feature of the predicted shock structure is the presence of hot macroscopic filaments whose formation is driven by reconnection along the equatorial plane. We argue that these compact plasma structures (giant plasmoids) may explain the mysterious knots contained within the Crab Nebula inner ring.

*Speaker

1. The particle acceleration conundrum in relativistic shocks

Relativistic shocks convert bulk mechanical energy of a relativistic flow into heat and non-thermal particles. They are believed to form at e.g., pulsar wind termination shocks, in gamma-ray bursts during the afterglow phase, and at the hotspots that terminate relativistic jets in AGN and possibly microquasars. Relativistic shocks are prime candidates to explain efficient particle acceleration inferred from the broadband non-thermal emission observed in these astrophysical systems and as such, they have drawn considerable interests and efforts of the community to understand the underlying acceleration mechanism (see e.g., [1]). Today, the consensus is that particle acceleration operates via the scattering of particles multiple times across the shock front. This process is well modeled by the first-order Fermi acceleration mechanism. It requires a high level of turbulence in both the upstream and downstream media to scatter particles efficiently.

In unmagnetized relativistic shocks, strong plasma turbulence is seeded by the Weibel instability. In this case, particle-in-cell (PIC) simulations show that particle acceleration is efficient, a steep power-law tail forms and the maximum energy steadily increases with time [2]. However the acceleration process is slow, and the extent of the power law only increases with the square-root of time. More importantly, it was shown later on that the maximum achievable energy sensitively depends on the upstream plasma magnetization $\sigma = B^2/(4\pi\Gamma nm_{\rm e}c^2)$, where B is the magnetic field, Γ is the bulk Lorentz factor, and n the plasma density. Even a low magnetization ($\sigma \lesssim 10^{-3}$) suffices to drastically limit the particle acceleration efficiency [3]. Above $\sigma \gtrsim 10^{-2}$, the magnetic field becomes dynamically important and quenches particle acceleration entirely [4]. This important result stems from the perpendicular nature of relativistic shocks (magnetic field lines are perpendicular to the shock normal). If the shock is magnetized, particles are tied to the field lines and advected in the downstream flow, hence inhibiting any chance for the particles to return to the shock and initiate the Fermi process.

Therefore, except maybe for gamma-ray burst afterglows where $\sigma \sim 10^{-9}$, relativistic shocks are unable to account for efficient particle acceleration in astrophysical systems. This is particularly problematic in pulsar wind nebulae, where current models estimate the plasma magnetization to be of order unity in the Crab Nebula (e.g., [5]). Yet, these objects are the perfect examples of efficient accelerators. How to alleviate the above difficulties in the presence of a strong transverse field? We propose that the key to this conundrum lies in the anisotropic nature of pulsar wind termination shocks, and that the problem must be solved at a global scale to understand particle acceleration. In this contribution, we highlight our recent findings based on ab-initio PIC simulations performed with the `Zeltron` code of anisotropic shocks [6, 7], and we discuss their implications in the context of pulsar wind nebulae.

2. Particle acceleration at anisotropic shocks

2.1 Setup

The numerical setup is inspired from standard shock formation techniques, which consists of bouncing a cold beam of plasma off a perfectly reflecting wall (e.g., [2]). The reflected beam interacts with the incoming flow (the upstream medium) and a shock forms. The initial plasma is cold and drifts with a relativistic bulk velocity $V = 0.99c$. It is composed of electrons and
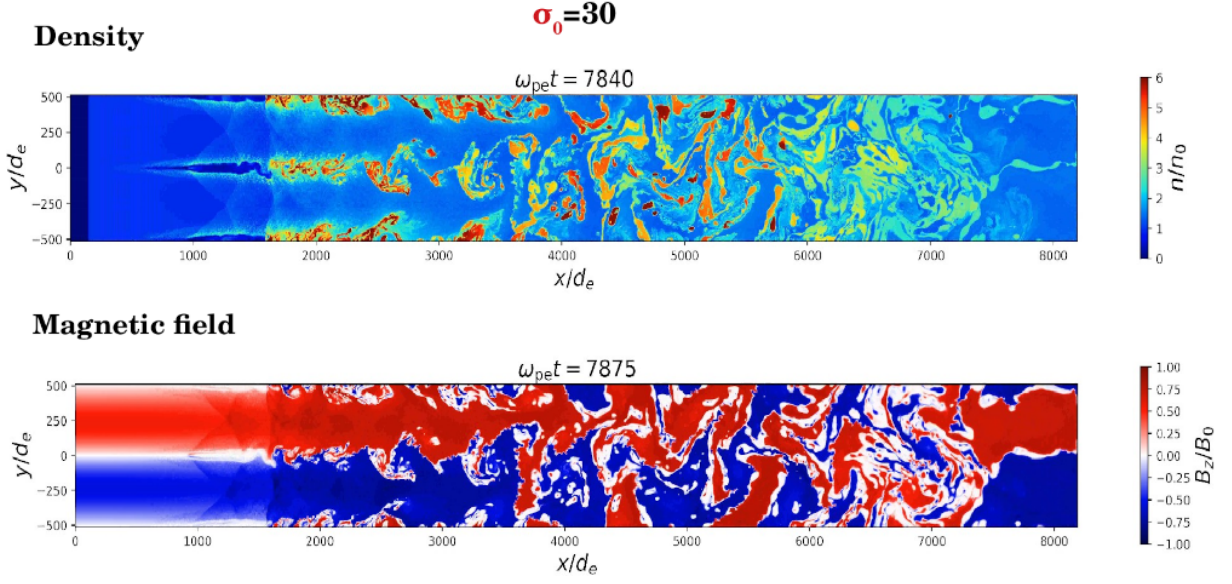
Figure 1: Total plasma density (top) and amplitude of the transverse magnetic field (bottom) at the late stages of the simulation for a fiducial upstream magnetization $\sigma_0 = 30$ or averaged magnetization $\langle \sigma \rangle \sim 5$.

positrons. The upstream field is composed of a perfectly perpendicular magnetic component, B_z, that is transverse to the 2D plane of the simulation. The essential difference with previous studies is the latitudinal evolution of the field strength, a good proxy is given by

$$B_z = B_0 \tanh\left(\frac{y}{L_s}\right) \sin\theta, \tag{1}$$

where B_0 is the fiducial magnetic field strength, L_s is the scale height over which the magnetic field reverses sign along the equatorial plane (this scale is related to the inclination of the pulsar magnetic axis), and $\theta = \pi(y + L_y)/2L_y$ mimics the polar angle in this Cartesian setup, and L_y is the system size. The field vanishes at the equatorial plane ($y = 0$) and at the poles ($y = \pm L_y$). The magnetic field is accompanied with an ideal transverse electric field, $\mathbf{E} = -\mathbf{V} \times \mathbf{B}/c$. The non-uniform magnetic profile implies that the upstream plasma must carry a non-zero current density, $\mathbf{J} = c\nabla \times \mathbf{B}/4\pi \neq \mathbf{0}$, and thus the upstream plasma must be initialized with care.

2.2 Overall shock structure and evolution

In the early phases, the shock structure is well described by previous works: a strong Weibel-dominated shock is created along the low-σ equatorial plane and at the poles, while a weak turbulence-free shock forms in high-σ regions at intermediate latitudes. At later stages (about one light box crossing time), the local approximation breaks down and the evolution of the shock significantly departs from previous results. A powerful back flow towards the upstream medium appears along the equatorial regions in the downstream flow, which in return excites Kelvin-Helmholtz vortices at the interface between highly- and weakly-magnetized regions. A thin large-scale current sheet forms along the equatorial plane to accommodate for the sharp reversal of the downstream magnetic field profile. The current sheet kinks but keeps its integrity on a scale of order the system size L_y. It is then torn apart by the Kelvin-Helmholtz instability at larger scales,
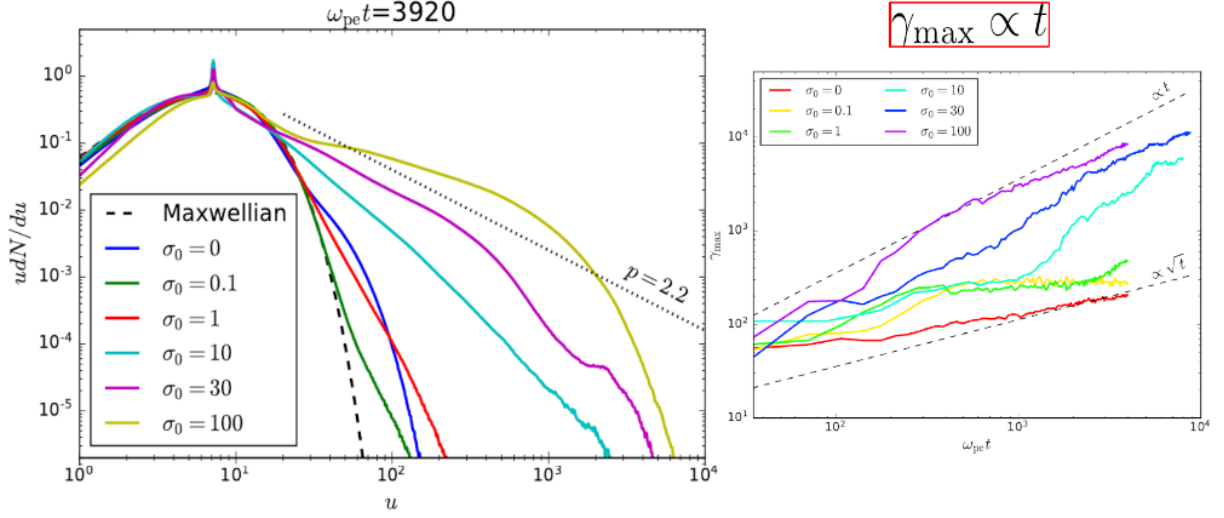
Figure 2: Total particle spectrum (left) and time evolution of the high-energy spectral cutoff (right) as a function of the upstream magnetization, where $u = \beta\gamma$ is the particle 4-momentum divided by $m_e c$, and ω_{pe} is the fiducial plasma frequency.

leading to a fully turbulent downstream flow (see Figure 1). At this stage, all latitudes are fully coupled and the global aspect of the problem takes its full meaning. Figure 1 shows another new striking feature of such shocks: it clearly appears as a spear-headed shape cavity drilling through the upstream medium along the equatorial plane. Its size increases with time without any sign of saturation within the duration of the simulation [6].

2.3 Particle spectra and acceleration mechanism

Figure 2 shows the astonishing efficiency of these shocks with respect to the unmagnetized case, the most effective shock known to accelerate particles so far. The total particle spectrum presents a hard power law, whose index hardens with increasing magnetization, reaching about $dN/d\gamma \propto \gamma^{-2}$ at the highest magnetization. As for the maximum cutoff energy, it increases linearly with time in contrast to uniform shocks. Thus, particle acceleration proceeds under the most favorable conditions (i.e., in the Bohm regime). The study of a large sample of particle trajectories reveals that two main acceleration patterns emerge. In both cases, the particle is first energized when it is captured by a current sheet. Magnetic reconnection abruptly accelerates particles above the background fiducial energy and serves as an injection mechanism to the following acceleration history of the particle that dominates at longer times. In the first case, the particle is then scattered in the turbulent downstream flow where the large-scale current layer has been disrupted into multiple turbulent structures. The acceleration history is reminiscent of a second-order Fermi acceleration as found in recent kinetic turbulence studies (e.g., [8]). This pattern explains the bulk of the particle acceleration history in the simulation. In the second case, we observe that the particle remains near the cavity at the shock front. The particle follows a relativistic Speiser orbit and samples the large-scale velocity shear. It appears that particle energization results from a genuine interplay between reconnection and macroscopic shear-flow acceleration. Although subdominant, this acceleration pattern explains alone the origin of the highest-energy particles in the simulation.
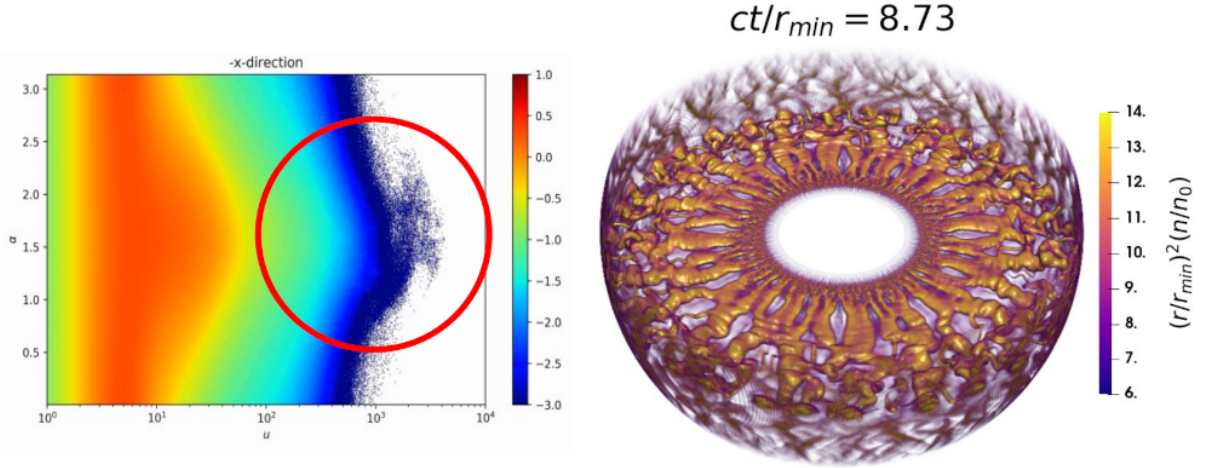
Figure 3: Left: Energy-resolved (4-momentum u) particle angular distribution (viewing angle α in radian, $\alpha = \pi/2$ for an observer looking along the equatorial plane). Right: Reconnection-driven filaments in the downstream flow of a 3D spherical simulation at time $ct/r_{\min} = 8.73$, where $r_{\min}$ is the inner radius of the simulation domain.

2.4 Crab gamma-ray flares and origin of the inner-ring knots?

Figure 3 presents the energy-resolved particle angular distribution. It shows that the highest-energy particles form a collimated beam against the incoming flow (i.e., moving along the $-x$-direction, red circle on the left panel). This component is also variable due to kinks of the equatorial current layer at the base of the shock-front cavity, leading to intermittent radiation in the highest-energy band only. This is a natural outcome of anisotropic shocks. Interestingly, these properties are reminiscent of the puzzling Crab gamma-ray flares [9]. Another byproduct of this particle acceleration scenario is the formation of large-scale plasma filaments, or giant plasmoids, along the equatorial plane in 3D simulations (right panel in Figure 3). The fragmentation of the current layer is driven by the tearing instability and the reconnection process. The non-linear evolution of this instability leads to an inverse cascade phenomena: small-scale plasma filaments merge in a hierarchical manner to produce a dozen macroscopic structures on a system size scale that are filled with particles energized by reconnection. We propose that these filaments could explain the mysterious X-ray knots visible along the Crab Nebula inner ring (e.g., [10]).

3. Summary and perspectives

Relativistic magnetized shocks are very efficient particle accelerators, provided that their global (i.e., boundary conditions) and anisotropic nature are accounted for. The feedback from large scales dramatically changes the structure of the shock and tightly couples all latitudes together. Plasma turbulence is driven by current-driven and Kelvin-Helmholtz instabilities. Together, they mediate efficient particle acceleration in the form of a second-order Fermi acceleration in the downstream turbulent flow and reconnection/shear acceleration for the most energetic particles. The latter mechanism operates at the Bohm rate, and thus offers a promising way to accelerate particles to the highest energies in pulsar wind nebulae, and in particular the Crab and its mysterious gamma-ray

flares, one of the few PeVatrons identified in the Galaxy. Another important consequence of this work applies to the termination shock of relativistic jets in AGN and microquasars (in particular SS433). If the acceleration mechanism still holds in these environments, it may accelerate particles up to Hillas criterium energies, meaning ultra-high energies in AGN jets and lobes.

Acknowledgments

References

[1] Marcowith, A., et al., 2016. The microphysics of collisionless shock waves. Reports on Progress in Physics 79, 046901.

[2] Spitkovsky, A. 2008. Particle Acceleration in Relativistic Collisionless Shocks: Fermi Process at Last?. The Astrophysical Journal 682, L5.

[3] Sironi, L., Spitkovsky, A., Arons, J. 2013. The Maximum Energy of Accelerated Particles in Relativistic Collisionless Shocks. The Astrophysical Journal 771, 54.

[4] Gallant, Y. A., et al. 1992. Relativistic, Perpendicular Shocks in Electron-Positron Plasmas. The Astrophysical Journal 391, 73.

[5] Porth, O., Komissarov, S. S., Keppens, R. 2014. Three-dimensional magnetohydrodynamic simulations of the Crab nebula. Monthly Notices of the Royal Astronomical Society 438, 278.

[6] Cerutti, B., Giacinti, G. 2020. A global model of particle acceleration at pulsar wind termination shocks. Astrophysical & Astrophysics 642, A123.

[7] Cerutti, B., Giacinti, G. 2021. Formation of giant plasmoids at the pulsar wind termination shock: A possible origin of the inner-ring knots in the Crab Nebula. Astrophysical & Astrophysics 656, A91.

[8] Zhdankin, V., Werner, G. R., Uzdensky, D. A., Begelman, M. C. 2017. Kinetic Turbulence in Relativistic Plasma: From Thermal Bath to Nonthermal Continuum. Physical Review Letters 118, 055103.

[9] Abdo, A. A., et al. 2011. . Science 331, 6018.

[10] Hester, J. J. 2008. The Crab Nebula : an astrophysical chimera. Annual Rev. Astron. Astrophys. 46, 127.